(13) Immirzi, A. *Acta Crystallogr., Sect. B* **1980**, *B36*, 2378.
(14) See, e. g.: Tadokoro, H. In *Structure of Crystalline Polymers*; Wiley: New York, 1979.
(15) Hall, M. M., Jr. *J. Appl. Crystallogr.* **1977**, *10*, 66.
(16) Klug, H. P.; Alexander, L. E. In *X-ray Diffraction Procedures*; Wiley: New York, 1974.
(17) Brückner, S.; Porzio, W. *Makromol. Chem.*, in press.
(18) French, A. D., Gardner, K. H., Eds. *Fiber Diffraction Methods*; ACS Symposium Series 141; Americal Chemical Society: Washington, DC, 1980. Symposium on Polymer Diffraction, Philadelphia, 1984: *J. Macromol. Sci., Phys.* **1985-1986**, *B24*, 1-4.

Solvent Dependence of Energy Trapping in Methacrylic Acid–Vinylphenanthrene Block Copolymers

Keiko Kamioka and S. E. Webber*

Department of Chemistry and Center for Polymer Research, University of Texas at Austin, Austin, Texas 78712

Yotaro Morishima

Department of Macromolecular Science, Faculty of Science, Osaka University, Toyonaka, Osaka 560, Japan. *Received July 8, 1987*

ABSTRACT: Steady-state and time-dependent fluorescence studies have been carried out on A–B–A block copolymers in which A = methacrylic acid and B = 9-vinylphenanthrene. The length of the B block greatly modifies the fluorescence properties of the polymer, especially in poorer solvents. In particular energy trapping at a weakly bound excimer site increases along the solvent sequence DMF, DMF/methanol, methanol. For a given solvent the energy trapping increases in the order of the degree of polymerization of the vinylphenanthrene sequence. A simple coil simulation lattice model with excitation random walk was studied in order to understand the experimental results on a molecular level. While the model is crude, it implies that the time-dependent fluorescence is most dependent on density of traps and the excitation transfer time and weakly dependent on the number of intracoil contacts.

Introduction

The study of photophysical processes of polymers with pendent aromatic chromophores has been quite active in recent years. In general these are complex systems with a wide range of local conformations of neighboring groups, energy trapping via excimer formation, and down-chain energy transfer. In the present paper we report the results of detailed fluorescence studies of methacrylic acid (MA) (A)–9-vinylphenanthrene (VPh) (B) A–B–A block copolymers (1) which have been studied previously by Morishima et al.[1] Our objective is to elucidate the relationship between the nature of a solvent and the extent of energy trapping and energy transfer within the phenanthrene blocks. In particular we attempt to ascertain if cross-chain energy migration occurs in this system by comparing our photophysical studies with a simple lattice model of the polymer chain. We carry out this comparison by using a "fractal" expression for the fluorescence decay function

$$I(t) = \exp(-at^{\tilde{d}/2} + bt^{\tilde{d}} - t/\tau_0) \qquad (1)$$

in which $\tilde{d}$ is the so-called "spectral" dimension and τ_0 is the unperturbed lifetime of the chromophore. This expression is based on a random walk to traps distributed on a lattice.[2] The spectral dimension may vary between 1 (ideal 1-D) and 2 (ideal 3-D). For the case of a phenanthrene block of ca. 43 units we find $\tilde{d}$ to vary from 1.08 to 1.4 as the solvent is changed from DMF (good solvent for the phenanthrene) to methanol (poor solvent for the phenanthrene). This variation is consistent with the idea that the phenanthrene block undergoes a transition from a random coil to a compact coil of higher effective dimensionality (e.g. significant numbers of non-nearest-neighbor phenanthrene contacts).

Although monomeric phenanthrene does not form excimers in concentrated solution, phenanthrene groups tethered together on short chains[3] or pendent to polymer chains[4] have been reported to exhibit an excimer-like fluorescence which is less red-shifted relative to that of the monomer than for many other "classical" aromatic excimers (e.g. naphthalene, pyrene). We find the same type of fluorescence feature in the present experiments, the intensity of which is solvent-dependent. We assign this solvent dependence to the density of excimer forming sites (efs). It is these sites that we believe act as traps for the mobile monomeric excitation. Thus the solvent quality is thought to modify the effective dimensionality of energy migration and the density of the efs. It is not possible at present to deconvolute uniquely these two effects. One complication is that the efficiency of populating the excimer as measured by steady-state spectroscopy is higher than measured by the monomer lifetime shortening. This situation is normally referred to as "static quenching", which means simply that there exists a sensitization process that is faster than can be measured in the fluorescence decay.

Table I
Degree of Polymerization of Block Copolymer

sample	DP_{MA}–DP_{VPh}–DP_{MA}
B-VPh-43	77–43–77
B-VPh-16	53–16–53
B-VPh-7	23–7–23
R-VPh-21[a]	

[a] Random copolymer of VPh and MA (Ph content 21 mol %).

Experimental Section

(a) Materials. MA–VPh–MA block copolymers and a VPh–MA random copolymer were prepared by Y. Morishima et al. at Department of Macromolecular Science, Osaka University, Osaka, Japan.[1] Table I lists the block and random copolymer samples used in the present study.

N,N-Dimethylformamide (DMF) was purified by fractional distillation. Methanol (Fisher Scientific Certified A.C.S. Spectranalyzed) was used as received. All solutions used for

0024-9297/88/2221-0972$01.50/0

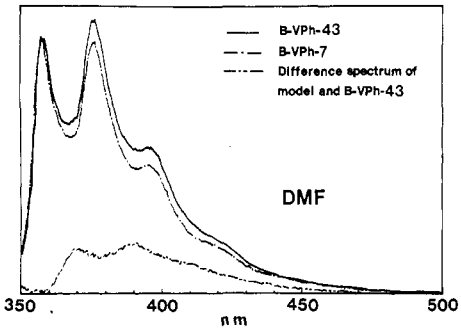

Figure 1. Steady-state fluorescence of B-VPh normalized at 358 nm and the indicated difference spectrum (see text). Solvent: DMF.

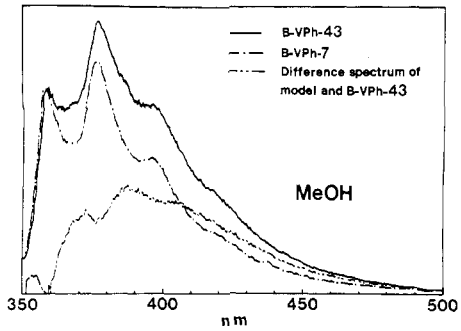

Figure 2. Steady-state fluorescence of B-VPh normalized at 358 nm and the indicated difference spectrum (see text). Solvent: methanol.

fluorescence experiments were filtered through 0.2 μm (TPFE) filters (Millipore) and sonicated in order to remove any aggregates. Solutions were bubbled for ca. 15 min. with N_2 to remove dissolved O_2 before all fluorescence experiments.

(b) Fluorescence Measurement. All steady-state fluorescence spectra were taken on a SPEX FLUOROLOG 2.

Fluorescence lifetimes were measured by using a Photochemical Research Associates correlated single-photon counting apparatus. Excitation pulses (~2.5-ns fwhm) were generated by a Model 510 B nanosecond flash lamp filled with air at ca. 350 Torr. The excitation wavelength (316-nm nitrogen line) and the emission wavelength were selected by two Instruments S.A. Model H-10 monocromators. The detector was a thermoelectrically cooled Hamamatsu R928 photomultiplier. A LeCroy Model 3501 24 bit analog-to-digital converter was used to digitize the TAC output into histogram memory of a LeCroy 3500M multichannel analyzer. These data were transferred to the University of Texas Cyber system and fitted to exponential decay functions using reconvolution techniques.[5] In this technique the value of χ^2 is minimized for the quantity

$$\chi^2(k) = \int_0^{t_{max}} |I_{obsd}(t) - \int_0^t F(t-\tau;k) R_{obsd}(\tau)\, d\tau|^2 w(t)\, dt \qquad (2)$$

where $I_{obsd}(t)$ is the experimentally observed fluorescence at time t, $R_{obsd}(\tau)$ is the experimentally observed response function of the excitation lamp and detector combination, and $F(t-\tau;k)$ is a proposed fluorescence decay function with parameter(s) k (all values normalized to a maximum value of unity). The weighting function $w(t)$ is taken to be $I_{obsd}(t)^{-1}$. The integral in eq 2 is actually a summation over all the data channels. In addition to minimizing the quantity $\chi^2(k)$ with respect to variations in k, the residuals

$$D(t) = \left(I_{obsd}(t) - \int_0^t F(t-\tau;k) R_{obsd}(\tau)\, d\tau\right) w(t) \qquad (3)$$

were inspected for randomness.

Results

(a) Steady-State Fluorescence. Fluorescence spectra of B-VPh-43 and B-VPh-7 in DMF and MeOH are shown in Figures 1 and 2 (the spectrum of 1:1 DMF/MeOH is essentially intermediate between these two cases). The spectra are normalized at 358 nm. Fluorescence spectra of block copolymers are slightly broadened compared with that of the random copolymer, although no clear excimer emission in the longer wavelength region is observed in any solvent. When the polarity of the solvent increases, the fluorescence spectra of block copolymers become broader and the relative intensity at longer wavelengths increases. For R-VPh-21, there is no significant change in spectra, but when the polarity of the solvent increases, the spectra tend to red-shift by 1–2 nm. In the case of the block copolymers no red-shift is observed. A new broad emission spectrum having maximum around 390 nm was obtained by subtracting the R-VPh-21 spectra from block copolymer spectra. The intensity of this new feature decreases in the order of B-VPh-43 > B-VPh-16 > B-VPh-7 and MeOH > 1:1 MeOH/DMF > DMF. Clearly this feature is unlike the classical excimer fluorescence observed in many polymer systems. Nevertheless we ascribe it to a "trapping state" since no corresponding feature is observed in the absorption or excitation spectra.

Table II
Fluorescence Quantum Yields[a]

sample	ϕ^M_{fl}	ϕ^D_{fl}	ϕ_{fl}	$\bar{\tau}_M$[b]
(a) DMF				
B-VPh-43	0.030	0.008	0.0380	15.7
B-VPh-16	0.034	0.006	0.040	18.0
B-VPh-7	0.045	0.009	0.053	18.1
R-VPh-21			0.160	38.5
(b) 1:1 DMF/MeOH				
B-VPh-43	0.022	0.010	0.032	13.3
B-VPh-16	0.030	0.008	0.038	15.8
B-VPh-7	0.032	0.007	0.039	16.3
R-VPh-21			0.156	32.0
(c) MeOH				
B-VPh-43	0.010	0.010	0.020	7.0
B-VPh-16	0.013	0.008	0.021	7.9
B-VPh-7	0.020	0.009	0.029	11.9
R-VPh-21			0.081	25.9

[a] Determined by comparison of corrected spectra to phenanthrene in cyclohexane (ϕ_{fl} = 0.13). [b] See eq 3 and 4—$\tau_M = \sum a^M_i \tau^M_i$.

The fluorescence quantum yield was determined for these three polymers by comparing the relative areas of corrected spectra with monomeric phenanthrene and based on the value of ϕ_{fl} = 0.13 for phenanthrene in cyclohexane.[6] The separation of the block polymer fluorescence into a monomer and excimer fraction permits the estimation of the individual quantum yields (Table II). We note the following: (1) the total fluorescence yield (ϕ_{fl}) for R-VPh-21 is very similar to monomeric phenanthrene except in MeOH it is halved; (2) ϕ_{fl} is much lower for the block polymers than either the random copolymer or monomeric phenanthrene, and it is ϕ_{fl}^M (monomer quantum yield) that decreases systematically with the length of the phenanthrene block or with decreasing solvent quality. The decrease in ϕ_{fl}^M is not compensated for by an increase in ϕ_{fl}^D along this series. In fact within experimental error ϕ_{fl}^D is essentially constant. This implies that energy trapping at the emitting excimer site is not the only quenching process but rather one must evoke trapping at a nonemitting excimer site (which is equivalent to classical "self-quenching").

For comparison we have also listed the values of $\bar{\tau}$ in Table II. This weighted lifetime is given by

$$\bar{\tau}_M = \int_0^\infty I_{fl}^M(t')\, dt' \qquad (4)$$

$$\bar{\tau}_M = \sum a_i^M \tau_i^M$$

Table III
Multiexponential Fits to Fluorescence Decay at 358 nm

solvent	type	τ_1, ns/a_1	τ_2, ns/a_2	τ_3, ns/a_3	$\bar{\tau}_M$,[c] ns
(a) B-VPh-43					
DMF	100 ns	1.8/0.156	11.1/0.457	26.8/0.387	15.7
	100 ns; const	3.7/0.245	14.7/0.455	28.5/0.300[a]	16.1
DMF/MeOH	100 ns	1.7/0.152	7.2/0.465	25.2/0.383	13.3
MeOH	50 ns	1.9/0.523	7.4/0.307	17.2/0.170	6.2
	100 ns	2.9/0.459	6.7/0.400	21.1/0.141	7.0
	50, 100 ns; global	2.4/0.501	7.5/0.372	21.0/0.127	6.7
	50 ns; const	1.8/0.530	8.8/0.414	28.5/0.057[a]	6.2
	100 ns; const	3.7/0.708	12.4/0.241	28.5/0.051[a]	7.1
(b) B-VPh-16					
DMF	100 ns	4.1/0.178	10.9/0.341	28.1/0.481	18.0
	100 ns; const	3.7/0.179	11.2/0.362	28.5/0.460[a]	17.8
DMF/MeOH	100 ns	2.9/0.256	13.1/0.467	32.3/0.277	15.8
MeOH	50 ns	1.3/0.481	6.6/0.377	21.3/0.142	6.1
	100 ns	3.2/0.615	9.3/0.250	27.0/0.135	7.9
	50, 100 ns; global	1.6/0.469	7.2/0.423	28.1/0.108	6.8
	50 ns; const	0.6/0.564	6.9/0.371	28.5/0.065	4.9
	100 ns; const	3.1/0.617	10.0/0.266	28.5/0.116	7.9
(c) B-VPh-7					
DMF	100 ns	3.0/0.193	9.3/0.289	28.7/0.518	18.1
	100 ns; const	3.7/0.179	11.2/0.362	28.5/0.459[a]	17.9
DMF/MeOH	100 ns	2.6/0.243	14.1/0.421	29.0/0.335	16.3
MeOH	50 ns	3.4/0.602	16.1/0.376	20.1/0.022	8.5
	100 ns	3.8/0.477	11.1/0.279	28.5/0.244	11.9
	50, 100 ns; global[b]	5.5/0.769	10.6/0.017	29.3/0.214	10.7
	50 ns; const	2.2/0.448	9.6/0.366	28.5/0.112[a]	8.4
	100 ns; const	3.9/0.510	12.0/0.250	28.5/0.240[a]	11.8
(d) R-VPh-21					
DMF	200 ns	12.7/0.159	43.4/0.841		38.5
DMF/MeOH	200 ns	14.3/0.179	35.9/0.821		32.0
MeOH	200 ns	14.0/0.359	32.6/0.641		25.9

[a] Constrained lifetime. [b] Not a satisfactory fit. [c] Equation 4.

where the explicit form in eq 4 assumes a multiexponential for the time-dependent fluorescence decay of the monomer and it is assumed that $I_{fl}(0) = 1$. We have found that this quantity is much more stable to duplicate data sets etc. than the individual a_i, τ_i components. $\bar{\tau}_M$ has a direct physical significance since it is a measure of the fluorescent quantum yield. It is seen that $\bar{\tau}_M$ does not decrease as rapidly as ϕ_{fl}^M, which implies a very rapid trapping process (so-called "static quenching") that can not be detected with our ca. 1-ns time resolution. The time dependence of the fluorescence will be discussed in more detail in the next subsection.

(b) Time-Dependent Fluorescence. Most fluorescence decay curves were monitored at 358 nm since the excimer makes essentially no contribution at this wavelength. The fluorescence decay is nonexponential for all samples and all solvents, including R-VPh-21. This is commonly found for polymers, partially as a consequence of a range of local environments and the complex photophysics of trapping etc. There are certain clear-cut experimental observations that do not require deconvolution: (1) the monomer fluorescence decay is faster for the longer chain block copolymer; (2) the poorer the solvent quality the faster the monomer fluorescence decay. These observations are illustrated in Figure 3 for DMF and MeOH. We note that in the good solvent there is only a small difference between the decay curves but that these differences are accentuated for the poor solvent (MeOH).

The random copolymer also displays sensitivity to solvent, with $\bar{\tau}_M(\text{MeOH})/\bar{\tau}_M(\text{DMF}) \cong 0.67$ while $\phi_{fl}^M(\text{MeOH})/\phi_{fl}^M(\text{DMF}) \cong 0.51$ (see Table II). We presume this difference to be the result of "self-quenching" within the random copolymer without yielding any corresponding excimer fluorescence. The fact that $\bar{\tau}_M$ and ϕ_{fl}^M is so much smaller for the block copolymers than the random copolymer is ascribed to the more facile energy transfer and high density of excimer forming sites in the former.

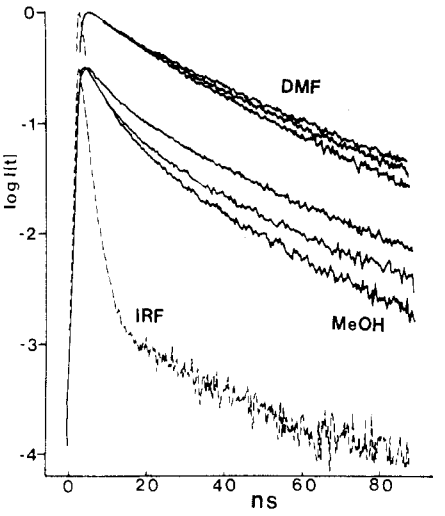

Figure 3. Fluorescence decay for B-VPh-7, B-VPh-16, and B-VPh-43 (from upper to lower trace for solvent indicated). All curves for a given solvent have been superimposed at their maxima for ease of comparison (IRF = instrument response function; wavelength observed 358 nm).

Evaluating quantitatively the form of the time-dependent fluorescence decay function can be quite difficult since the analysis requires a convolution of a proposed fitting function with the instrument response function (see eq 2). One of the most general forms for the fitting function is a sum of exponentials

$$I_{fl}(t) = \sum a_i e^{-t/\tau_i} \qquad (5)$$

where for our fits we constrain $\sum a_i = 1$ (all decays normalized to unity at the maximum). For a given sample the set of best fit a_i, τ_i will depend on the time scale over

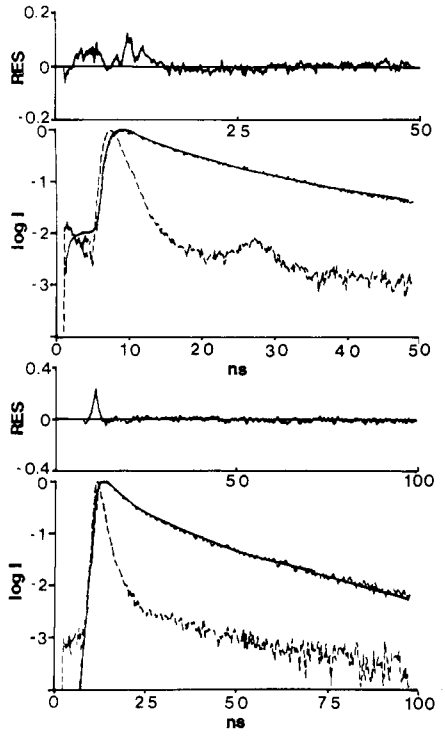

Figure 4. Example of a simultaneous fit of fluorescence decay for two different time scales (see text) for B-VPh-43 in MeOH.

which the fluorescence decay is measured since the fluorescence decay is not precisely described by eq 5. Thus in Table III is presented the values of a_i, τ_i for several different kinds of fits: (1) for the time scale indicated (either 50 or 100 ns), (2) "global" (fit both the time scales simultaneously) (see Figure 4), (3) constrain one τ_i to be 28.5 ns. This latter value was chosen because this lifetime showed up consistently in the longer time fits for B-VPh-7 and might be thought to correspond to the lifetime of a vinylphenanthrene block without traps. As can be seen, the individual components of the multiexponential may vary significantly according to the time scale of the data or the exact method of fitting. However $\bar{\tau}_M$ is rather consistent ($\bar{\tau}_M$ for B-VPh-7 shows the largest variation with fit) and the change in $\bar{\tau}_M$ with solvent is well outside its sensitivity to fitting method.

For purposes of comparison with "fractal theory", the monomer fluorescence was also fit to a fractional power expression given by eq 1, taking τ_0 = 28.5 ns (see above). The parameters of the fit were not terribly sensitive to the choice of τ_0. We have previously used an expression like (1) (except constrained to b = 0) for fitting a system in which simultaneous energy migration and trapping occurs.[7] By and large this type of function seems to be as well-behaved as a multiexponential fitting function like (5). In the present system the quality of fit greatly increased if the $t^{\tilde{d}}$ term was included in (1) which we interpret to be the result of a smaller distance of energy transfer (i.e. more nearly constrained to nearest neighbor transfers). Equation 1 provided a satisfactory fit only for the B-VPh-43 block polymer in the sense that the parameters a, b, and $\tilde{d}$ varied in a sensible way with solvent. We presume that this is the result of finite size effects which are not properly reflected in eq 1. We will come back to this point in the Discussion.

It is difficult to know exactly how accurate the fitting parameters in eq 1 are. For τ_0 = 28.5 ns and b constrained to its best value (the fits are not terribly sensitive to b) one may plot χ^2 (eq 2) as a function of $\tilde{d}$ and a. An example of this is presented in Figure 5 for MeOH. The uncertainty

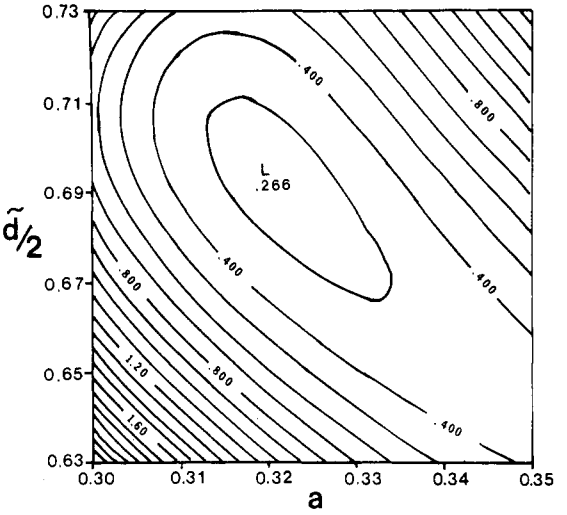

Figure 5. Topographic representation of χ^2 as a function of $\tilde{d}/2$ and a (see text).

Table IV
Fractal Fitting Parameters for B-VPh-43[a]

solv	$\tilde{d}$	a	b^b
DMF	1.08[c]	0.165[c]	0.005
DMF/MeOH	1.13 (±0.04)	0.240 (±0.005)	0.011
MeOH	1.39 (±0.04)	0.320 (±0.010)	0.009

[a] $I_{fl}(t) = \exp(at^{\tilde{d}/2} + bt^{\tilde{d}} - t/\tau_0)$ with τ_0 constrained to 28.5 ns. [b] Fit not very sensitive to b so meaningful uncertainty value not calculable. [c] χ^2 is not a symmetric minimum around best fit—estimate of uncertainty inaccurate.

in the parameters presented in Table IV are estimated from the first contour around the minimum for this type of topographical plot. As is seen in Table IV, the parameters a (proportional to the density of traps) and $\tilde{d}$ (the spectral dimension) increase systematically as the solvent quality decreases.

Discussion: A Simple Lattice Model

(a) Coil Generation. Generation of a self-avoiding walk on a lattice is a simple way to represent a polymer coil if one is not concerned with the details of pendent group interaction. Since our observations have a natural distance scale on the order of the phenanthrene–phenanthrene Förster radius (ca. 0.9 nm), we believe such a simple representation can serve to model some of the time-dependent properties of simultaneous energy transfer and trapping.[8] There exists a number of analytical approaches to this latter problem that have been developed primarily for shorter time regimes[9] (primarily applied to fluorescence depolarization). We will report more detailed calculations in future publications using a different method of simulating the time-dependent solutions.[10] However in all solutions to the time-dependent problem one must propose a model for the set of transfer rates between chromophores, which is what we describe in this subsection.

Polymer coils were simulated on a computer by self-avoiding-random walks on a simple cubic lattice following the method of Rosenbluth and Rosenbluth[11] and McCrackin et al.[12] The first step of the walk is from (0,0,0) to (0,0,1); before each later step of the walk, each possible direction for the step is examined for intersection with previous steps. A list of all directions which do not cause intersection is made. A random choice of the allowed steps is made, and a step is then in the chosen direction. When all six possible new positions are occupied, the process is then terminated and a new coil must be generated, starting again from (0,0,0).

Because the above scheme does not generate all self-avoiding walks with equal probabilities, each walk must be weighted separately when the averages of the parameters over many walks are calculated. Let s be the maximum number of choices for step of the walk without immediate reversals; $s = 5$ for the simple cubic lattice. When two positions of the walk not connected by a single step lie a distance equal to the lattice spacing from each other, they are said to form a contact. Let the ith step of a walk form C_i contact. In the above described method of generating the walks, a random choice for the ith step is made of these possible directions; each choice has a priori probability $1/(s - C_i)$. The first step may be taken in $s + 1$ direction. Thus the probability of generating a particular walk is

$$\text{prob} = 1/(s+1)\prod_{i=2}^{N} 1/(s - C_i) \tag{6}$$

the weight of the walk is the reciprocal of the probability and so is given by

$$w = (s+1)\prod_{i=2}^{N}(s - C_i) \tag{7}$$

For a sample of m walks, the weight of the kth walk is then

$$w_k = (s+1)\prod_{i=2}^{N}(s - C_{ik}) \tag{8}$$

In a calculation for polymer walks with nearest-neighbor interaction energies, the average over parameters of the walks are multiplied by Boltzmann factors

$$\alpha_i = \exp(-P_i\Phi) \tag{9}$$

where $\Phi = \epsilon/(kT)$. In eq 9 P_i is the total number of contacts in the kth walk, ϵ is the energy per contact, k is the Boltzmann constant, and T is the temperature. The estimate of the average value of any calculated property v of the walk is

$$\langle v \rangle = \sum_{k=1}^{m} v_k w_k \alpha_k / \sum_{k=1}^{m} w_k \alpha_k \tag{10}$$

where v_k is value of the parameter for the kth walk.

In order to determine the values of parameters for walks with large attraction energies (large value for Φ), importance sampling described by McCrackin et al.[12] was used. This method gives different probabilities to steps taken away from or toward the origin of the random walk. For example, consider a walk on a cubic lattice started at the lattice site (0,0,0) and after a number of steps reaches the lattice site (3,−5,−4). Let the next steps of the walk that are allowed by volume exclusion be $\Delta x = 1$, $\Delta x = -1$, $\Delta y = 1$, $\Delta z = 1$, and $\Delta z = -1$. Without importance sampling, each of these steps would have the probability of $^1/_5$ of being chosen. However, if steps taken toward the coordinate (0,0,0) are given twice the probability of those taken away from (0,0,0), the above steps will have probabilities of $^1/_8$, $^1/_4$, $^1/_4$, $^1/_4$, and $^1/_8$, respectively. By properly selecting the probabilities the sampling of coils that are energetically favored (see eq 9) is much more efficient. The best choice of these probability factors for a given Φ value has to be determined by trial and error.

The proper weights, w_k, will no longer be given by eq 8 but are easily computed. For any step in a walk, let there be s allowable steps. Let a multiplicity m_j ($j = 1$–s) be assigned to each step proportional to the probability of the step. For the above example, $m_j = 1$ or 2. In general, the probability of step is

$$m_c / \sum_{j=1}^{s} m_j \tag{11}$$

Table V
Relation of $\langle R^2 \rangle$, L, and ϵ/kT for Coil Generation Model

L	$\Phi = \epsilon/kT$	$\langle R^2 \rangle$	n_c
7	0.275	9.1	1.91
	0.5	6.7	1.99
16	0.275	24.5	2.27
	0.5	12.9	2.46
43	0.275	67.4	2.54
	0.5	29.6	2.87

Where m_c is multiplicity of the chosen step. The probability of a given N step walk is then

$$\text{prob} = \frac{1}{6}\prod_{i=2}^{N}(m_{ci} / \sum_{j=1}^{s} m_{ji}) \tag{12}$$

and the weighting factor is

$$w = 6\prod_{i=2}^{N}(\sum_{j=1}^{s} m_{ji}/m_{ci}) \tag{13}$$

Of most direct importance to our simulation of energy transfer and trapping is the average number of nearest neighbors ($\bar{n}_c$, number of "contacts") and the density of excimer forming sites. Obviously we expect both of these to increase as the coil density increases. The former can be directly counted from the simulation and have been compiled in Table V along with $\langle R^2 \rangle$ for several choices of ϵ/kT. For the lowest L (the length of phenanthrene block) value (7) the effect of the ends is particularly noticed since $\bar{n}_c$ is less than 2 (the mole fraction of ends is 2/7). However for larger L the value of $\bar{n}_c$ is greater than 2 and increases slightly as the "solvent quality" decreases. As we will see, this slight increase in contacts leads to some shortening in the predicted time dependence.

Our lattice units correspond to an energy transfer distance (ca. 1 nm) and hence may contain several chromophores of the physical system. Alternatively one can allow the time simulation to permit other than nearest-neighbor energy-transfer steps. These extensions will be considered in later publications.

(b) Simulations of Time Dependence. These simulations were carried out by an explicit random walk between points on the computer generated polymer coil that are separated by one lattice spacing. If X_T is the mole fraction of trapping sites, then the average number of traps per coil is $\bar{n}_T = X_T L$. These are assumed to be Poisson distributed on the individual lattices, such that the probability of n_T traps is given by

$$P(n_T) = (\bar{n}_T)^{n_T} \exp(-\bar{n}_T)/n_T \tag{14}$$

The positions of the n_T traps are picked by a random number generator. Likewise the lattice position of the initial excitation is random.[13] The excitation is allowed to move between neighboring lattice sites until trapping occurs. In some simulations the excitation was allowed to detrap with a certain probability, although this addition did not seem to improve the qualitative fit of the simulations to the experimental data. If $F(t)$ is the survival probability of the excitation at time t, based on trapping only, then the observed fluorescence intensity should obey

$$I_{fl}(t) \propto F(t) \exp(-t/\tau_0) \tag{15}$$

where τ_0 is the normal fluorescence lifetime. Thus the appearance of $I_{fl}(t)$ depends on (1) the density of traps, (2) the energy-transfer time ("hopping time", τ_h) relative to τ_0, (3) the average number of intrapolymer contacts, and (4) the length of the lattice. These are listed in approximately descending order of importance to the appearance

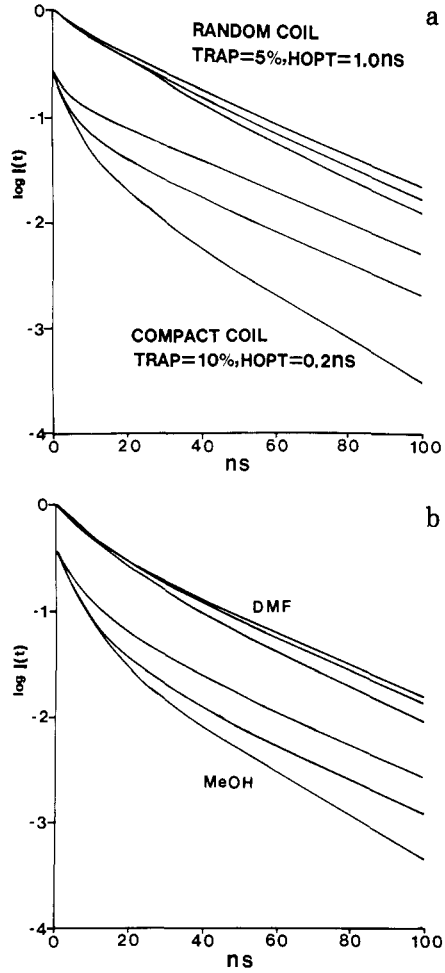

Figure 6. a. Simulation of fluorescence decay for "compact coil" (Φ = 0.5) and "random coil" (Φ = 0.275) for chain length 7, 16, and 43 (from top to bottom). b. Experimental decay curves deconvoluted from single-photon lifetime data (chain length ordering like panel a).

of the decay curve, although the last two parameters are obviously correlated with each other.

As expected the decay curves from these simulations are nonexponential. For a given value of ϵ/kT the rate of decay increases rapidly with trap density and $(\tau_h)^{-1}$. This is illustrated in Figure 6a for chains of length 7, 16, and 43 (recall however the earlier comment that there may be more than one chromophore per lattice site). The dependence on the lattice length is accentuated at smaller values of τ_h as one might expect from the ability of the excitation to sample a larger number of contacts, including the relatively infrequent nonneighboring ones. The fluorescence decay function deconvoluted from the data in Figure 3 for DMF and MeOH is plotted in Figure 6b for comparison. Note that the simulation results presented in Figure 6a were selected to most closely resemble the experimental decays of Figure 6b. However in no sense was there an attempt to obtain a best fit of the model to experiment.

We have attempted to fit our experimental data to a fractional time expression (eq 1), and we have carried out the same fitting procedure to the simulation data (except the "response function" is a δ function at t = 0). The parameters a, b, and $\tilde{d}$ are presented in Table VI for different choices of trap density, τ_h, and coil size for L = 43. As expected $\tilde{d}$ increases slightly as the coil decreases in size. The constant a increases by almost a factor of 2 as the trap density is doubled as one would expect intuitively. The b parameter also increases with trap density.

Table VI
Fit of Eq 1 to Simulation Data (L = 43, τ_0 = 28.5 ns, τ_h = 0.05 ns)

trap concn %	$\langle R^2 \rangle$	$\tilde{d}$	a	b
5	75.8	1.134	0.381	0.021
5	36.8	1.266	0.364	0.018
5	22.0	1.290	0.375	0.019
10	72.0	1.190	0.666	0.036
10	38.5	1.236	0.723	0.035
10	23.0	1.290	0.687	0.030

The basic idea behind this expression is as follows: if p is the mole fraction of traps on a lattice, then after n *unique* steps on the lattice the survival probability is

$$F(n) = (1 - p)^{n-1} \tag{16}$$

(this assumes that the excitation has not been started at a trapping site). $F(n)$ may be averaged over the ensemble of initial positions of the excitation with respect to traps. If λ is defined by

$$\lambda = -\ln (1 - p) \tag{17}$$

then

$$\langle F(n) \rangle = \langle e^{-\lambda(n-1)} \rangle$$

$$F(n) = \exp[\sum_{j=i}^{\infty} K_j(-\lambda)^j/j!] \tag{18}$$

where K_j is the jth cumulent average of the distribution of unique steps taking by the excitation. In particular

$$K_1 = \langle n \rangle \tag{19}$$

$$K_2 = \langle n^2 \rangle - \langle n \rangle^2 \equiv \sigma_n \tag{20}$$

If p is small then $\lambda \cong p$. Truncating (18) after the two leading terms yields

$$\langle F(n) \rangle = \exp[-p\langle n \rangle + p^2\sigma_n/2] \tag{21}$$

It has been proposed[2] for a fractal geometry that

$$\langle n \rangle \cong (t/\tau_h)^{\tilde{d}/2} \tag{22}$$

$$\sigma_n \cong K\langle n \rangle^{\tilde{d}} \tag{23}$$

where t/τ_h represents the number of steps taken in time t and $\tilde{d}$ is the so-called "spectral dimension". Equation 22 is exact for 1-D lattices ($\tilde{d}$ = 1) in the limit of $\langle n \rangle$ large. For ideal 3-D lattices $\tilde{d}$ = 2. Thus for disordered lattices we expect $\tilde{d}$ to lie in the range 1–2.

The above treatment implicitly assumes that the number of unique sites visited by the excitation grows without limit with t which is not the case for finite lattices. Additionally we have assumed a Poisson distribution of traps such that for short chains there is a significant probability that there are no traps. We find that eq 1 is not able to fit the decay curves for L = 7 at all and L = 16 only marginally.

(c) Comparison of Simulations to Experimental Results. Because of the complex interplay of the parameters of the simulation a unique fit to experiment is probably unrealistic at this stage. The most important characteristics of the experimental results are (1) more rapid decay in solvents of poorer quality, (2) a more pronounced molecular weight effect in poorer solvents, and (3) extreme nonexponentiality.

The simulations for 5 mol % trap, τ_h = 1 ns, and Φ = 0.275 are rather similar to experiment (Figure 6) for DMF (good solvent). Increasing the trap density or decreasing τ_h results in too large a molecular weight effect and too rapid decay. The difference between compact or random coils is minimal.

For the experimental results in MeOH the best qualitative fit for $L = 43$ is for 10 mol % trap, $\tau_h = 0.2$ ns and $\Phi = 0.5$ (Figure 6). The simulations do not seem to fit the experimental results for $L = 7$ for any choices we have made. In general the simulations underestimate the rate of decay. We are inclined to the view that our model is simply not adequate for these very short chains. This could be for a variety of reasons: (1) the relatively large importance of the ends, (2) the fact that R_0 for phenanthrene self-transfer is a significant fraction of $\langle R^2 \rangle^{1/2}$ for this polymer, and (3) the overestimation of the fraction of short chains that are trap free using the Poisson distribution (traps can be formed dynamically during the singlet state lifetime).

How reasonable are our estimated hopping times derived from these simulations? If we use the Förster expression

$$\tau_h = \tau_0 (l/R_0)^6 \tag{24}$$

where l is the average chromophore–chromophore separation, then for $l = 0.5$ nm, $\tau_h = 0.98$, ns and for $l = 0.4$ nm, $\tau_h = 0.26$ ns. These are in reasonable agreement with the values derived from the simulations for DMF and MeOH "fits" respectively, but there is very strong dependence of τ_h on l in expression 24. Also the R_0 used in (24) assumes randomization of the orientation of a pair of chromophores on a time scale that is fast compared to the transfer rate. For random orientations of static chromophores R_0 is modified by a factor of ca. 0.945.[14] Ng and Guillet[15] have studied in detail the fluorescence decay of poly[(9-phenanthryl)methyl methacrylate] copolymerized with (9-anthryl)methyl methacrylate which acts as a long-range energy trap. They estimate the singlet migration rate between phenanthrenes to be 1.5×10^{-5} cm^2/s in 77 K glasses. If one uses a simple 1-D diffusion constant expression

$$\Lambda_s = l^2/2\tau_h \tag{25}$$

then for $l = 0.4$ and 0.5 nm, respectively, one estimates $\tau_h = 0.05$ and 0.08 ns. Thus to the extent these two phenanthrene systems can be compared, there would seem to be quite a range of plausible τ_h values. Most likely these estimates of τ_h in all cases suffer from the crudeness of the theoretical model and the fact that in the physical systems there is a broad range of τ_h values depending on the particular chromophore pair.

Summary

Our experimental observations demonstrate that for phenanthrene block polymers diminishing the solvent quality enhances the formation of a lower energy emitting species which we assign to a weakly bound excimer state. While the monomeric singlet state lifetime is shortened by this trapping state, the lifetime shortening is only approximately half that expected from the decrease in monomer fluorescence yield. This could be the result of "static quenching" which occurs on a shorter time scale than our instrumental resolution or could imply a fundamental change in the transition dipole moment of the phenanthrene. On the basis of the similarity of the absorption spectra and shape of the monomeric component of the fluorescence spectra for block and random copolymers, we favor the former interpretation.

We have attempted to simulate the time dependence of systems of this type by generating a coil on a cubic lattice with different $\langle R^2 \rangle$ values and then carrying out a simple random walk calculation. We have assumed (1) energy transfer only between chromophores on neighboring lattice sites (not necessarily bonding) and (2) a Poisson distribution of traps. While it is not valid to speak of "fitting the experimental data" with such a crude model, the most important parameters seem to be trap density and excitation hopping times. While the number of nonbonding contacts does affect the decay rate, this effect is relatively minor. It is seen that collapsing the coil does lead to a slight increase in the "spectral dimension" ($\bar{d}$) as one would expect. However it is by no means obvious that polymers may be treated as fractal objects with respect to electronic energy transfer. These relations will be the subject of later publications.[16]

Acknowledgment. S.E.W. would like to acknowledge the financial support of the National Science Foundation (DMR-834755) and Materials Research Grant (DMR-841806) and the Robert A. Welch Foundation (F-356). This work was supported in part as a Japan–U.S. Cooperative Research Project "Cooperative Photoconversion and Photosynthesis Research". Y.M. wishes to acknowledge the Grant-in-Aid for Scientific Research (No. 59430019) from the Ministry of Education, Science and Culture, Japan.

Registry No. (Methacrylic acid)(9-vinylphenanthrene) (block copolymer), 112863-61-3.

References and Notes

(1) (a) Morishima, Y.; Hashimoto, T.; Itoh, Y.; Kamachi, M.; Nozakura, S. *Makromol. Chem., Rapid Commun.* **1981**, *2*, 507. (b) Morishima, Y.; Itoh, Y.; Hashimoto, T.; Nozakura, S. *J. Polym. Sci., Polym. Chem. Ed.* **1982**, *20*, 2007.
(2) (a) Zumofen, G.; Blumen, A.; Klafter, J. *J. Chem. Phys.* **1985**, *82*, 3198. (b) Klafter, J. *J. Phys. Lett.* **1984**, *45*, 49.
(3) Zachariasse, K.; Busse, R.; Schrader, U.; Kuhnle, W. *Chem. Phys. Lett.* **1982**, *89*, 303.
(4) (a) Morishima, Y.; Kobayashi, T.; Nozakura, S. *J. Phys. Chem.* **1985**, *89*, 4081. (b) Tamai, N.; Masuhara, H.; Matuga, N. *J. Phys. Chem.* **1983**, *87*, 4461.
(5) A recent discussion of this technique has been presented by D. Phillips and I. Soutar in *Photophysical and Photochemical Tools in Polymer Science, Conformation, Dynamics and Morphology*; Winnik, M. A. Ed.; NATO ASI Series; D. Reidel: Dordrecht, 1986. Also see: *Time Correlated Single Photon Counting*, O'Connor, D. V., Phillips, D. Academic: 1984. Demas, J. N. *Excited State Lifetime Measurements*; Academic: New York, 1983.
(6) Berlman, I. B. *Handbook of Fluorescence Spectra of Aromatic Molecules*; Academic: New York, 1971.
(7) Bai, F.; Chang, C.-H.; Webber, S. E. *Macromolecules* **1986**, *19*, 2484.
(8) For a recent review of this problem in the context of polymer photophysics see: Frank, C. W.; Fredrickson, G. H.; Andersen, H. C. In *Photophysical and Photochemical Tools in Polymer Science*; Winnik, M. A., Ed.; NATO ASI Series; D. Reidel: Publishing Co., 1986; pp 495–522.
(9) (a) Ediger, M. D.; Dominque, R. P.; Peterson, K. A.; Fayer, M. D. *Macromolecules* **1985**, *18*, 1182. (b) Peterson, K. A.; Zimmt, M. B.; Linse, S.; Dominque, R. P.; Fayer, M. D. *Macromolecules* **1987**, *20*, 168.
(10) Friedrichs, M. S.; Friesner, R. A. *Chem. Phys. Lett.* **1987**, *137*, 285.
(11) Rosenbluth, M. N.; Rosenbluth, A. W. *J. Chem. Phys.* **1955**, *23*, 356.
(12) McCrackin, F. L.; Mazur, J.; Guttman, C. M. *Macromolecules* **1973**, *6*, 859.
(13) If the initial excitation position is a trapping site, this corresponds to instantaneous quenching and no further steps are taken.
(14) The orientation factor (K^2) for chromophores that rotate rapidly during their fluorescence lifetime is $^2/_3$. For a random ensemble of static dipoles $K^2 = 0.475$. Thus the multiplicative factor is $(0.475/(^2/_3))^{1/6}$. See: Berlman, I. B. *Energy Transfer Parameters of Aromatic Compounds*; Academic: New York, 1973; p 28.
(15) Ng, D.; Guillet, J. E. *Macromolecules* **1982**, *15*, 728.
(16) Byers, J.; Friedrichs, M.; Friesner, R.; Webber, S. E. *Efficient Numerical Simulation of the Time-Dependence of Electronic Energy Transfer in Polymers. 1. Short Range Transfer and Trapping*; manuscript in preparation.